International Journal of Nanomedicine

Dovepress
open access to scientific and medical research

Open Access Full Text Article

ORIGINAL RESEARCH

Enhancement of physicochemical properties of nanocolloidal carrier loaded with cyclosporine for topical treatment of psoriasis: in vitro diffusion and in vivo hydrating action

This article was published in the following Dove Press journal:
International Journal of Nanomedicine
28 March 2017
Number of times this article has been viewed

Siti Hajar Musa[1]
Mahiran Basri[1]
Hamid Reza Fard Masoumi[1]
Norashikin Shamsudin[2]
Norazlinaliza Salim[1]

[1]Department of Chemistry, Faculty of Science, [2]Department of Medicine, Faculty of Medicine and Health Sciences, Universiti Putra Malaysia, Serdang, Malaysia

Abstract: Psoriasis is a chronic autoimmune disease that cannot be cured. It can however be controlled by various forms of treatment, including topical, systemic agents, and phototherapy. Topical treatment is the first-line treatment and favored by most physicians, as this form of therapy has more patient compliance. Introducing a nanoemulsion for transporting cyclosporine as an anti-inflammatory drug to an itchy site of skin disease would enhance the effectiveness of topical treatment for psoriasis. The addition of nutmeg and virgin coconut-oil mixture, with their unique properties, could improve cyclosporine loading and solubility. A high-shear homogenizer was used in formulating a cyclosporine-loaded nanoemulsion. A D-optimal mixture experimental design was used in the optimization of nanoemulsion compositions, in order to understand the relationships behind the effect of independent variables (oil, surfactant, xanthan gum, and water content) on physicochemical response (particle size and polydispersity index) and rheological response (viscosity and *k*-value). Investigation of these variables suggests two optimized formulations with specific oil (15% and 20%), surfactant (15%), xanthan gum (0.75%), and water content (67.55% and 62.55%), which possessed intended responses and good stability against separation over 3 months' storage at different temperatures. Optimized nanoemulsions of pH 4.5 were further studied with all types of stability analysis: physical stability, coalescence-rate analysis, Ostwald ripening, and freeze–thaw cycles. In vitro release proved the efficacy of nanosize emulsions in carrying cyclosporine across rat skin and a synthetic membrane that best fit the Korsmeyer–Peppas kinetic model. In vivo skin analysis towards healthy volunteers showed a significant improvement in the stratum corneum in skin hydration.

Keywords: cyclosporine, nanoemulsion, mixture experimental design, psoriasis, Ostwald ripening, Franz diffusion cell, transepidermal water loss

Introduction

Psoriasis is a T-cell-mediated autoimmune inflammatory skin disease that manifests in such symptoms as skin-surface inflammation, epidermal proliferation, hyperkeratosis, angiogenesis, and abnormal keratinization.[1] As for psoriatic skin, the mitotic activity of basal keratinocytes is 50-fold compared to normal skin activity. Therefore, keratinocytes of psoriatic skin have only 3–5 days to be removed from the basal layer to the cornified layer (28–30 days for normal skin).[2] This limited period, accompanied by rapid differentiation activity, causes the dead skin to be accumulated on the skin's surface, resulting in a thick and dry skin surface. More simply, psoriasis presents as thick patches of red, dry, and itchy skin. Treatments can only help to reduce and relieve

Correspondence: Mahiran Basri
Department of Chemistry, Faculty of Science, Universiti Putra Malaysia, 43400 Serdang, Selangor, Malaysia
Tel +60 3 8946 7807
Email mahiran@upm.edu.my

submit your manuscript | www.dovepress.com
Dovepress
http://dx.doi.org/10.2147/IJN.S125302

the problems, not cure them. The current standard treatment for managing psoriasis includes topical therapy as first-line treatment for mild disease, followed by phototherapy and systemic (or oral) therapy for more severe disease.[3]

Systemic therapy includes methotrexate, acitretin, cyclosporine, and antibody therapy. Methotrexate is the oldest and the most common oral treatment for psoriasis. However, its short-term side effect of bone marrow toxicity can lead to death.[4] Methotrexate needs to be prescribed with caution considering the patient's condition with regard to obesity, diabetes, and heavy alcohol intake, due to the increase risk of liver fibrosis.[5] Similarly with oral acitretin, it results in cheilitis (lip cracking), alopecia (hair loss), xerosis (dry skin), myalgia (muscle pain), rhinitis (symptoms affecting the nose), epistaxis (bleeding nose), skin peeling, slow wound healing, and sticky skin.[6]

In the current therapeutic armamentarium, cyclosporine is one of the standard oral medications used for moderate–severe psoriasis. Cyclosporine ($C_{62}H_{111}N_{11}O_{12}$) was originally extracted from the fungus of *Tolypocladium inflatum* Gams in 1971.[7] It consists of neutral cyclic peptides with eleven amino acids, which lead the cyclosporine molecule to become a highly lipophilic substance.[8] Cyclosporine is a type of immunosuppressant that acts selectively and inhibits the activation of T cells from mediating skin inflammation.[9] Clinically, cyclosporine is available in the form of soft gelatin capsules or an oral solution containing preconcentrates under the name of Sandimmune®. Since this product shows bile-dependent absorption and exhibits significant intra- and interpatient variability, a new formulation, Neoral®, that is delivered orally was developed. Oral cyclosporine gives rise to significant undesirable side effects in patients that include nephrotoxicity, cardiotoxicity, hypertension, and hepatotoxicity.[10] Direct interaction of cyclosporine with inner organs could worsen arterial hypertension and increase insulin resistance, as well as interfere with fatty-acid metabolism, inducing dyslipidemia and hyperuricemia.[11] Therefore, in order to avoid problems affecting the inner organs, topical therapy could be the best alternative.[12]

Topical therapy remains the main therapeutic regimen, whether or not patients require any other additional treatments. More than 50% of patients have been reported to use topical treatment compared to only 6% using systemic therapy.[13] Many current topical treatments for psoriasis focus on the usage of steroidal anti-inflammatory drugs, such as hydrocortisone, betamethasone dipropionate, and triamcinolone acetonide.[14] However, topical corticosteroid cannot be used for long periods, as it can lead to tachyphylaxis, whereby medication that is highly effective initially would progressively lose efficacy with prolonged use.[15] Malik et al reported that steroidal drugs caused decolorization of the skin and skin thinning, followed by easy bruising, even with minimum shear.[16] Other current topical therapies include dithranol (anthralin), vitamin D analogues (calcipotriol), retinoid (tazarotene), coal tar, and tacrolimus with salicylic acid. Penetration enhancers, such as salicylic acid, give burning, stinging, and skin-peeling effects.[17] Though many options are offered by topical treatment, such complications as staining, bad odor, side effects, and difficulty in application have limited their usage.[15,18] Malik et al has reported hijama as a traditional topical treatment for treating psoriasis. However, this treatment is not very practical, since it needs to be performed in aseptic conditions by a well-trained hijama physician.[16]

Nanocolloidal carriers, also known as nanoemulsions, consist of two immiscible phases with droplet size 20–500 nm.[19] The use of nanoemulsions in the pharmaceutical industry, specifically for topical application, has been proven to be better compared to other delivery carriers, such as suspension and gels.[20] Two different phases (lipophilic and hydrophilic) enable nanoemulsions to be used as nanocarriers to carry highly lipophilic/hydrophilic components to the specific targeted area. Nanoemulsion systems containing the oil phase carrying lipophilic molecules that act as polar lipids would help in maintaining the barrier integrity of the stratum corneum and thus make penetration through the skin barrier easier.[21] Even though cyclosporine is a highly hydrophobic molecule, its large molecular weight (1,202.64 Da) would restrict entrance through the skin barrier. Therefore, a nanoemulsion could overcome this restriction with extremely small vehicles.

Nutmeg oil (NMO) is extracted from the dried seed of nutmeg fruit – *Myristica fragrans*. Major components of NMO consist of terpene hydrocarbon (such as sabinene, pinene, and limonene), terpene derivatives (such as copaene, asarone, and anthrone), and myristicin.[22] With almost 80% terpenes and 14% myristicin content, NMO has the unique property of possessing both antifungal and anti-inflammatory activities.[23] NMO has a very pleasant odor and aroma, which is suitable to be used for medication.

Virgin coconut oil (VCO) is obtained through a mechanical and natural process on dried of coconut kernels. It consists of 46%–48% lauric acids (C_{12}), together with other minor components, such as myristic acid (C_{14}), palmitic acid (C_{16}), and oleic acid ($C_{18:1}$).[24] VCO has been reported to have good moisturizing property and antibacterial activity toward skin.[25]

Nevin and Rajamohan discovered the ability of topical VCO in treating wounds of rat skin.[26] Therefore, utilizing VCO could enhance the efficacy of topical nanoemulsion treatment for the skin of psoriasis patients.

Traditionally, in optimization of mixture compositions, a method called "one factor at a time" is used to study the behavior of components involved in the formulation and preparation analysis. However, this method seems to be unreliable and inefficient for finding the optimal formulation and conditions.[27] As an alternative method, response surface methodology has been a useful tool in the optimization of many experiments. As part of this tool, mixture experimental design (MED) is a suitable approach to be used when numbers of variables are varying but total amounts of those formulations are fixed and constant.[28] Besides requiring fewer number of experiments and thus being more cost-effective, this approach could also allow a better understanding of relationships among independent variables (control variables) and responses (intended quality of variable).[29]

In this work, cyclosporine was used as an active ingredient, while VCO and NMO acted as the oil phase to be formulated into the nanoemulsion system, with which we aimed to enhance the effective topical psoriasis treatment. Optimization of nanoemulsion-formulation ingredients, such as the amount of oil, surfactant, xanthan gum, and water, was based on particle size, polydispersity index (PDI), viscosity, and consistency index (*k*-value) for rheological study.

Materials and methods

Materials

VCO was purchased from Manila Coco Bio-essence Inc (Muntinlupa, Philippines). NMO was prepared in our research laboratory. Polysorbate 80 (Tween 80) and xanthan gum were purchased from Sigma-Aldrich (St Louis, MO, USA). Phenonip was purchased from Clariant (Muttenz, Switzerland). Cyclosporine was purchased from Euroasian Chemicals (Mumbai, India). Water was deionized using a Milli-Q filtration system.

Solubility of cyclosporine

Cyclosporine (0.1%, w/w) was added to the NMO (15%, w/w). The mixture was stirred in a water bath at 30°C until all the cyclosporine was dissolved and a transparent NMO mixture observed. Another 0.1% (w/w) cyclosporine was added to the previous NMO–cyclosporine mixture until a clear transparent oil mixture was formed. The step of cyclosporine addition (0.1%, w/w) was repeated until a nontransparent and saturated form of NMO–cyclosporine mixture was observed. The total percentage of cyclosporine that was successfully dissolved in the clear transparent NMO was recorded as the highest amount of cyclosporine that can be dissolved in the oil. Similar steps were carried out for another two sets of oils: individual VCO and a mixture of NMO and VCO.

Mixture experimental design

A D-optimal MED was used to study the effect of nanoemulsion composition (oil content, surfactant content, xanthan gum content, and water content) on responses (particle size, PDI, viscosity, and *k*-value) using Design-Expert® software (version 7.0; Stat-Ease, Minneapolis, MN, USA). The software randomly listed 20 runs, with ten replicate formulations. This design allowed for the fitting of a full quadratic model, a check for lack of fit, and an estimate of experimental error. Four independent variables with low-limit and high-limit values were set as follows: oil content (X_1; 15%–30%, w/w), surfactant content (X_2; 10%–15%, w/w), xanthan gum content (X_3; 0.5%–1%, w/w), and water content (X_4; 52.3%–72.8%, w/w). Design constraints for the four independent variables were set to 98.3%, while the balance for the formulation was fixed to the amount of cyclosporine (1%) and phenonip as preservative. All experiments were carried out in random sequence to minimize the effects of unexplained variability in the actual responses due to extraneous factors.[30]

In the construction of the final model, a nonlinear response function was expected. Therefore, from the D-optimal MED, a quadratic model was chosen to interpret the data. The general equation for quadratic model design is as follows:

$$Y_i = \sum_{i=1}^{4} \beta_i x_i + \sum_{i=1}^{3} \sum_{j \neq i}^{4} \beta_{ij} x_i x_j + \varepsilon \quad (1)$$

where the coefficients β_i and β_{ij} represent the regression coefficients calculated from the experimental data by multiple regression. The generated model contains quadratic terms, which explain the nonlinear nature of responses, and multiple-factor terms explaining interaction effects between factors.[31]

Formulation of nanoemulsion

Cyclosporine (1%, w/w) was completely dissolved in a mixture of VCO and NMO at a ratio of 2:1 (w/w), followed by the addition of Tween 80 (10%–15%, w/w) into the same mixture. This mixture acted as the oil phase. Xanthan gum

(0.5%–1% w/w), which was used as thickening agent, was dissolved in deionized water (w/w), and this mixture acted as the aqueous phase. Both of these phases were heated in a warm-water bath at 30°C for 25 minutes. The temperature was set to 30°C to preserve the natural compounds of oils and cyclosporine. The aqueous phase was then further homogenized using an overhead stirrer (RW 20 digital; IKA, Staufen im Breisgau, Germany) for 5 minutes at a speed of 50 rpm, while the oil phase was homogenized using a high-shear homogenizer (Ultra-Turrax T25; IKA) for 5 minutes at a speed of 6,000 rpm. With the high-shear homogenizer, 15 mL volume of the nanoemulsion was formulated by dropwise addition of the aqueous phase into the oil phase. The nanoemulsion was mixed and sheared for 30 minutes at a speed of 10,000 rpm. In the process of emulsification, phenonip was added into the nanoemulsion as a preservative.

Verification of models

A triplicate sample of optimized nanoemulsion formulation was formulated and further analyzed with respect to response criteria. The experimentally determined values were compared with the predicted values obtained from the response regression equations.[32]

Particle size, PDI, and ζ-potential

The particle size, PDI, and ζ-potential of the nanoemulsion were measured using dynamic light scattering, scattered at an angle of 173° and a temperature of 25°C using a Nano ZS90 (Malvern Instruments, Malvern, UK). During sample preparation, the cyclosporine-loaded nanoemulsion was diluted using the standard sample-dilution procedure to prevent the overlapping of droplets during the measurement process. The diluted samples were kept at a count rate of less than 500 kcps (kilo count per second) to yield less scattering intensity and to avoid multiple scattering.[33] All measurements were repeated three times.

Rheology

Dynamic shear rheometry (Kinexus rotational rheometer; Malvern Instruments) was used to determine the rheological behavior of the formulated nanoemulsion. Shear rate ranged from 0.01 to 50 seconds at controlled temperature (25°C). Cone and plate geometry of 4°/40 mm was used, and the plate gap was set at 0.15 mm. After the sample had been placed on the plate, the instrument was equilibrated for 5 minutes before measurement was determined. From the 38 data points generated, the average viscosity result was recorded in Pascal seconds (Pa·s). The formulated nanoemulsion was analyzed with respect to its viscosity and *k*-value, which were fitted to the power-law model (Equation 2):

$$\eta = ky^{n-1} \tag{2}$$

where η is the viscosity (Pa·s), y the strain rate, k the consistency index of the nanoemulsion, and n is the power (shear thinning) index ($n<1$); the lower the n-value, the more shear thinning the nanoemulsion has.[34]

Nanoemulsion pH

Triplicates of optimized nanoemulsion formulations were prepared at pH 3.5. All nanoemulsions were stored at three different temperatures (4°C, 25°C, and 45°C) for a month. Their stability was determined based on appearance. Gravitational separation was reported as the percentage of cream layer using Equation 3:[35]

$$\%\,\text{cream layer} = \frac{\text{The height of cream layer}}{\text{The height of overall emulsion}} \times 100 \tag{3}$$

This procedure was repeated on different nanoemulsions of pH 4.5 and 5.5, where these pH values were the range reported to be suitable for a topical skin product.

Stability

For every optimized nanoemulsion formulation, triplicate samples were subjected to stability studies at three different temperatures (4°C, 25°C, and 45°C). The stability of the nanoemulsions was monitored through 3 months of storage with respect to particle size and appearance. Particle-size measurement was carried out for every 2 weeks of storage time.

Coalescence rate

Coalescence-rate study was conducted to identify the reason for particle-size changes over time. The collected particle-size data throughout the storage period for all temperatures were applied in the following equation (Equation 4):

$$\frac{1}{r^2} = \frac{1}{r_0^2} - \left(\frac{8\pi}{3}\right)\omega t \tag{4}$$

where r is the average radius after time, ω is the frequency of rupture per unit of the film surface and r_0 the value at time t=0. The rate of coalescence was determined by plotting the graph of $1/r^2$ against time, and a linear relationship was expected.

Ostwald ripening

Data on particle size for 3-month storage at different temperatures (4°C, 25°C, and 45°C) were collected. Ostwald ripening is an expansion of nanoemulsion particle size caused by the diffusion of the oil phase through the aqueous phase. The Lifshitz–Slesov–Wagner theory was used in determining the Ostwald ripening rate for each optimized nanoemulsion and the effect of storage temperature on this rate. The equation used for Ostwald ripening was:

$$\omega = \frac{dr^3}{dt} = \frac{8}{9}\left[\frac{C(\infty)\gamma V_m D}{\rho RT}\right] \quad (5)$$

where ω is the frequency of rupture per unit surface of the film, r the average radius of droplets over time, t storage time in seconds, $C(\infty)$ the bulk-phase solubility, V_m the molar volume of the internal phase, D the diffusion coefficient of the dispersed phase in the continuous phase, ρ the density of the dispersed phase, R the gas constant, and T the absolute temperature. Graphs of radii (nm^3) against storage time (seconds) at different temperatures were plotted and compared.

Freeze–thaw cycles

Triplicates of the optimized nanoemulsion formulation were placed at two different temperatures. Samples were first stored for 24 hours at 4°C, and then thawed at 25°C for 24 hours. This process was repeated three times (total of 6 days), and then samples were subjected to particle-size analysis.

In vitro diffusion

Determination of nanoemulsion diffusion through membranes was carried out using Franz diffusion cells (PermeGear, Hellertown, PA, USA). Franz diffusion-cell study commonly involves the use of excised animal skin or synthetic skin membrane. Both of these membranes function to demonstrate the diffusion rate of samples across human skin. This study was approved by the animal ethics committee of Universiti Putra Malaysia, Faculty of Medicine and Health Science (UPM/FPSK/PADS/BR-UUH/00415). Two main compartments of Franz cells are the donor and receptor medium. Between these two compartments was placed a 13 mm cellulose acetate membrane and rat-skin membrane. Both compartments were clipped tightly to ensure no sample leaking. This provided an area of 0.64 cm^2 for the diffusion of nanoemulsion between the media. On top of the donor compartment was placed 1 mL of cyclosporine-loaded nanoemulsion, while the receptor compartment contained 5 mL of phosphate-buffered saline (PBS; pH 7.4). During the process, the PBS sink condition was maintained at 37°C and stirred at a speed of 600 rpm. Every hour, 1 mL was taken out from the receptor compartment and another 1 mL of PBS inserted into the same compartment as a replacement. This maintained the total volume of 5 mL PBS inside the receptor compartment throughout the process. A total of five samples were collected over 5 hours. All experimental processes were carried out in triplicate.

The 1 mL sample that was taken out from the receptor compartment was mixed with 1 mL acetonitrile and analyzed by ultraviolet spectrometry at wavelength 320 nm. The collected data were analyzed with respect to percentage of cumulative cyclosporine detected in the receptor compartment. Three cyclosporine-loaded samples – Opt1, Opt2, and control (cyclosporine inside the ointment carrier) – were studied for diffusion for 1–3 hours, with all three samples containing the same cyclosporine loading (1%, w/w).

Kinetic release

Evaluation of kinetic release was carried out with respect to five kinetic models: zero-order, first-order, Higuchi, Korsmeyer–Peppas, and Hixson–Crowell. For each model, a graph was constructed based on the model's theoretical equation, as shown in Equation 6 (zero-order, percentage of cumulative drug released versus time), Equation 7 (first-order, log percentage of cumulative drug remaining versus time), Equation 8 (Higuchi model, percentage of cumulative drug released versus square root of time), Equation 9 (Korsmeyer–Peppas model, log percentage of cumulative cyclosporine released versus log time), and Equation 10 (Hixson–Crowell model, cube root of drug remaining versus time).[36] The best-fit equation was examined based on the coefficient of determination (R^2) value gained from the plotted graph. Model equations used were:

$$Q_0 - Q_t = k_0 t \quad (6)$$

$$\ln\left(Q_0/Q_t\right) = -k_1 t \quad (7)$$

$$Q_t = kt^{1/2} \quad (8)$$

$$Q_t/Q_\infty = kt^n \quad (9)$$

$$Q_0^{1/3} - Q_t^{1/3} = k_{HC} t \quad (10)$$

where Q_0 is the initial amount of cyclosporine in nanoemulsion, Q_t the amount of cyclosporine-loaded nanoemulsion permeated, k_0 the zero-order rate constant, k_1 the first-order

constant, k the constant reflecting the design variables of the system, Q_t/Q_∞ the fraction of drug released over time, n the release exponent, k_{HC} the Hixson–Crowell rate constant, and t the time.

In vivo skin

In vivo studies were focused on transepidermal water loss (TEWL) and water-content effect on healthy skin by the application of the formulated nanoemulsions (Opt1 and Opt2). A total of 15 healthy volunteers aged 20–35 years old (female) were quarantined for 1 hour at standardized temperature of 25°C±1°C and relative room humidity of 50%±3%. Initial readings of TEWL and moisture content for both forearms were taken using Tewameter® and Corneometer® dual MPA 580 (Courage-Khazaka, Cologne, Germany), respectively. Each nanoemulsion sample loaded with cyclosporine was then applied on both forearms, ensuring an identical covered area size (5×5 cm). The emulsion was left undisturbed for 3 hours on the skin area. After 3 hours, TEWL and moisture content were measured again and the reading used for the analysis. Ten readings were taken for every measurement set, and average data were recorded. The measurement process was carried out in triplicate. This study was conducted in accordance with the tenets of the Helsinki Declaration adopted by the World Medical Association in 2013, and complied with the International Conference on Harmonisation of Technical Requirements for Registration of Pharmaceuticals for Human Use-Good Clinical Practice. All participants provided written informed consent.

Statistical analysis

Analysis of variance (ANOVA), outlier detection, fitting of the second-order polynomial model, suggested formulation content, and graphical presentation in the form of ternary plot were determined using Design-Expert. The models were confirmed by analysis of goodness-of-fit correlation of determination (R^2) and verification of the regression model in terms of lack-of-fit test. Only significant ($P<0.05$) independent variables were chosen to be included in the model analysis. R^2 values need to be more than 0.8 in order to obtain an accurate model. Data are shown as mean ± standard deviation (n=3).

Results and discussion

Solubility of cyclosporine analysis

Oil-in-water emulsion provides the oil phase as the main medium in carrying the drugs to the targeted area. Therefore, it is very important for the drugs to be totally soluble in the oil phase to make sure that there is no drug leakage during the process. The mixture of NMO and VCO exhibited excellent solubility up to 1.5% (w/w) of cyclosporine in 15% (w/w) of total oil compared to the solubility of cyclosporine by individual oil: NMO up to only 0.5% (w/w) and VCO up to 1% (w/w). Mixture oil was proven to be a better choice in carrying and transporting higher amounts of cyclosporine compared to the individual oil. Mixture oil showed an increment in cyclosporine solubility, due to the higher content of fatty acids in the mixture solutions compared to the fatty-acid content in individual oil, and thus could solubilize more hydrophobic compounds.

Experimental design

D-optimal MED was employed to investigate the behavior of four responses that were influenced by four variables of the formulation composition. Table 1 shows the results obtained by 20 different compositions suggested by the software. With Design-Expert, it was shown that the quadratic model was well fitted with the experimental results for all responses. Criteria to be fulfilled in obtaining the best-fitted model were high *F*-value, low *P*-value (<0.05), insignificant lack of fit, high R^2, low standard deviation, a randomly scattered plot of residuals, and whether it was able to predict the validation set well.[31] Following are the equations that expressed the quadratic model for the prediction of particle size (Equation 11), PDI (Equation 12), viscosity (Equation 13) and *k*-value (Equation 14):

$$\begin{aligned} Y = {} & 431.91\,X_1 - 469.23\,X_2 + 105{,}600\,X_3 + 139.99\,X_4 \\ & + 69.08\,X_1X_2 - 115{,}000\,X_1X_3 - 47.47\,X_1X_4 \\ & - 97{,}184.75\,X_2X_3 + 502.78\,X_2X_4 - 107{,}400\,X_3X_4 \end{aligned} \quad (11)$$

$$\begin{aligned} Y = {} & 0.77\,X_1 + 0.044\,X_2 - 195.53\,X_3 + 0.26\,X_4 \\ & - 1.24\,X_1X_2 + 194.71\,X_1X_3 - 0.44\,X_1X_4 \\ & + 218.46X_2X_3 - 0.25X_2X_4 + 203.09X_3X_4 \end{aligned} \quad (12)$$

$$\begin{aligned} Y = {} & 14.34\,X_1 + 1{,}950.35\,X_2 + 100{,}700\,X_3 + 68.36\,X_4 \\ & - 2{,}093.73\,X_1X_2 - 93{,}762.83\,X_1X_3 + 101.71\,X_1X_4 \\ & - 105{,}900\,X_2X_3 - 2{,}459.77\,X_2X_4 - 100{,}900\,X_3X_4 \end{aligned} \quad (13)$$

$$\begin{aligned} Y = {} & 7.40\,X_1 + 158.86\,X_2 + 24{,}060.21\,X_3 + 8.14\,X_4 \\ & - 143.06\,X_1X_2 - 23{,}674.99\,X_1X_3 + 1.34\,X_1X_4 \\ & - 25{,}589.82\,X_2X_3 - 156.01\,X_2X_4 - 24{,}337.45\,X_3X_4 \end{aligned} \quad (14)$$

where X_1, X_2, X_3, and X_4 represent the independent variables of oil content, surfactant content, xanthan gum content and water content in w/w (%), respectively. Graphs of predicted

Table 1 Matrix of D-optimal MED: independent parameters and responses

Run	Independent parameters				Responses			
	X_1, oil content (%)	X_2, surfactant content (%)	X_3, xanthan gum content (%)	X_4, water content (%)	R_1, particle size (nm)	R_2, PDI	R_3, viscosity (Pa·s)	R_4, *k*-value
1	30.00	15.00	0.50	52.80	211.93	0.328	98.60	14.99
2	30.00	10.00	1.00	57.30	281.65	0.437	277.00	31.18
3	22.50	13.75	0.75	61.30	172.37	0.255	99.10	14.80
4	22.50	15.00	1.00	59.80	182.87	0.274	226.00	25.95
5	30.00	15.00	0.50	52.80	226.13	0.366	105.00	22.04
6	15.00	10.00	0.50	72.80	140.20	0.258	76.57	7.95
7	15.00	12.50	0.75	70.05	126.60	0.281	42.70	15.11
8	15.00	15.00	0.75	67.55	105.57	0.278	78.40	10.31
9	22.50	12.50	0.50	62.80	198.77	0.276	49.80	10.33
10	30.00	10.00	0.50	57.80	354.40	0.515	48.10	8.29
11	30.00	10.00	1.00	57.30	296.20	0.478	225.00	23.86
12	15.00	10.00	1.00	72.30	160.43	0.337	123.90	14.49
13	15.00	10.00	1.00	72.30	152.47	0.298	120.00	14.98
14	18.75	13.75	0.88	64.92	155.10	0.284	105.00	12.01
15	30.00	10.00	0.50	57.80	334.70	0.569	49.05	7.77
16	15.00	10.00	0.50	72.80	142.07	0.267	60.30	7.15
17	26.25	12.50	0.75	58.80	227.97	0.415	107.00	10.29
18	22.50	10.00	0.75	65.05	209.60	0.373	116.00	13.69
19	18.75	11.25	0.63	67.67	157.40	0.261	50.50	6.66
20	30.00	12.50	0.75	55.05	257.53	0.447	107.37	13.49

Abbreviations: MED, mixture experimental design; PDI, polydispersity index.

values (from the models) against the actual values (from the experiments) were plotted. All graphs for four significant responses showed high R^2 values for correlations between mixture contents.

Analysis of variance

ANOVA was studied based on the description of models obtained from the expressed quadratic equation. Table 2 shows that all four responses were significant ($P<0.05$), which explained the effect by changes in formulation composition. Each of the linear components (X_1, X_2, X_3, and X_4) influenced the responses with respect to their evaluation on the coefficients and *P*-value of the linear mixture.

Table 3 shows the regression coefficients for the four main responses R_1, R_2, R_3, and R_4. The tabulated data needed to be observed to make sure an accurate model was produced. The high R^2 values for all responses – R_1 (0.9941), R_2 (0.9531), R_3 (0.9828), and R_4 (0.8381) – explained the precision of the predicted data versus the actual data. Adequate precision is basically to measure the signal-to-noise ratio. Precision with value >4 indicates an adequate signal.[31] Therefore, the four responses fulfilled the intended requirement.

The quadratic model was the best-fitting model in analyzing the effect of independent variables on the chosen responses. Particle size (R_1) was most influenced by the interaction between X_1 and X_3 (oil content and xanthan gum content). PDI (R_2) and viscosity (R_3) were most likely to be influenced by interactions between X_1 and X_4 (oil content and water content) and X_2 and X_4 (surfactant content and water content), respectively.

Mixture experimental design analysis

Figure 1A shows the 3-D model for the interaction among all four independent variables toward particle-size response. As the amount of surfactant increased, particle size decreased. A similar trend was shown by the water-content effect, where the higher the water content, the smaller the particle size obtained. Surfactant functioned to provide coverage on the surface of oil droplets, keeping them from coming close together. As the amount of surfactant increased, this provided enough coverage of surfactant on the surface of the droplets. The higher the surfactant value, the higher the number of small droplets could be produced. Conversely, a low amount of surfactant would be insufficient to cover newly formed particles, allowing the merging of particles. This limitation leads to larger dispersed particles.[37]

However, in contrast to these two variables, the amount of oil and xanthan gum was directly proportional with the particle size obtained. Increasing the oil content or xanthan gum content increased the particle size formed. Increasing the concentration of the dispersed phase (oil content) in the

Table 2 ANOVA fitting quadratic model for four main responses

Response	Course	*F*-value	*P*-value	Data evaluation
R_1, particle size	Model	186.34	<0.0001	Significant
	Linear mixture	519.25	<0.0001	
	$X_1 X_2$	0.04	0.8473	
	$X_1 X_3$	10.17	0.0097	
	$X_1 X_4$	1.76	0.2143	
	$X_2 X_3$	7.70	0.0196	
	$X_2 X_4$	1.97	0.1903	
	$X_3 X_4$	9.44	0.0118	
	Lack of fit	0.26	0.9161	Not significant
R_2, PDI	Model	22.57	<0.0001	Significant
	Linear mixture	55.87	<0.0001	
	$X_1 X_2$	0.84	0.3807	
	$X_1 X_3$	2.07	0.1806	
	$X_1 X_4$	10.09	0.0099	
	$X_2 X_3$	2.60	0.1379	
	$X_2 X_4$	0.03	0.8611	
	$X_3 X_4$	2.25	0.1642	
	Lack of fit	1.15	0.4426	Not significant
R_3, viscosity	Model	38.02	0.0001	Significant
	Linear mixture	60.81	<0.0001	
	$X_1 X_2$	36.16	0.001	
	$X_1 X_3$	2.67	0.1532	
	$X_1 X_4$	9.75	0.0205	
	$X_2 X_3$	3.04	0.1317	
	$X_2 X_4$	61.22	0.0002	
	$X_3 X_4$	2.94	0.1372	
	Lack of fit	0.62	0.583	Not significant
R_4, *k*-value	Model	5.75	0.0057	Significant
	Linear mixture	13.06	0.0009	
	$X_1 X_2$	0.66	0.4349	
	$X_1 X_3$	1.81	0.2082	
	$X_1 X_4$	0.01	0.9421	
	$X_2 X_3$	2.11	0.1771	
	$X_2 X_4$	0.75	0.4066	
	$X_3 X_4$	1.91	0.1968	
	Lack of fit	1.66	0.2968	Not significant

Abbreviations: ANOVA, analysis of variance; PDI, polydispersity index.

nanoemulsion system caused flow resistance to increase, thus limiting the particle disruption process. This results in larger particle formation.[38] Xanthan gum, which acted as the thickening agent, was able to reduce homogenization efficacy, due to difficulty during the emulsification process.

Table 3 Regression coefficients for four main responses

	Response			
	R_1, particle size	R_2, PDI	R_3, viscosity	R_4, *k*-value
Standard deviation	7.40	0.03	5.93	3.73
PRESS	1,956.78	0.03	1,497.08	954.91
R^2	0.9941	0.9531	0.9828	0.8381
Adjusted R^2	0.9887	0.9109	0.9569	0.6924
Predicted R^2	0.9788	0.8284	0.8776	–0.1141
Adequate precision	45.686	14.119	17.004	7.333

Abbreviations: PDI, polydispersity index; PRESS, predicted residual error sum of squares.

Therefore, this resulted in the production of larger oil droplets in the nanoemulsion system.[39]

Figure 1B shows a 3-D model of the effect of independent variables on PDI. The lowest PDI was obtained at the lowest amounts of oil and xanthan gum, and also at the highest amounts of surfactant and water. PDI is a measurement of inconsistency in particle size in the nanoemulsion system, and PDI value is used as an indication to measure the uniformity of particle dispersion in the nanoemulsion system. Therefore, lower PDI values are favorable. In this case, the system formed was an o/w nanoemulsion, in which the particles being measured were the oil droplets. When a small amount of xanthan gum was used, the nanoemulsion formed became thinner. The homogenization process became easier, and led to more uniformed production of particle sizes, confirmed by a low PDI result.

Figure 1C shows the effect of components in the formulation on the viscosity of the nanoemulsion. From the results, it was found that formation of a more viscous nanoemulsion was influenced by increased oil and xanthan gum content. If a less viscous nanoemulsion were intended, a higher amount of surfactant and/or water was required. The viscosity trend was more likely dependent on the effect of the thickening agent and water content. Lapasin et al reported that xanthan gum that is soluble in water (aqueous phase) would form a gel network in the continuous phase.[40] This formed network keeps the water molecules from easily sliding from each other, providing a thicker feeling and viscosity to the nanoemulsion. The higher the water content, the more thickening agent was required in forming the gel network. Failure in providing sufficient quantity of thickening agent compared to the amount of water would definitely cause the viscosity of the nanoemulsion to reduce.

The *k*-value is the consistency coefficient obtained from the rheological equation, as described in Equation 2. Theoretically, the *k*-value should be in parallel with the viscosity-value trend. Figure 1D shows that the effect of independent variables on *k*-value was similar with the viscosity pattern. The optimum *k*-value (>10) was obtained with high oil and xanthan gum content, but at low surfactant and water content. Opt2 (13.69) had a higher *k*-value compared to Opt1 (10.25), in which greater value indicated better nanoemulsion structure.[41] From the collected results, it was verified that this constant value was in agreement with the viscosity of the nanoemulsion. Therefore, the formulated nanoemulsion system containing cyclosporine successfully fitted the power-law model with shear-thinning characteristics ($n<1$).

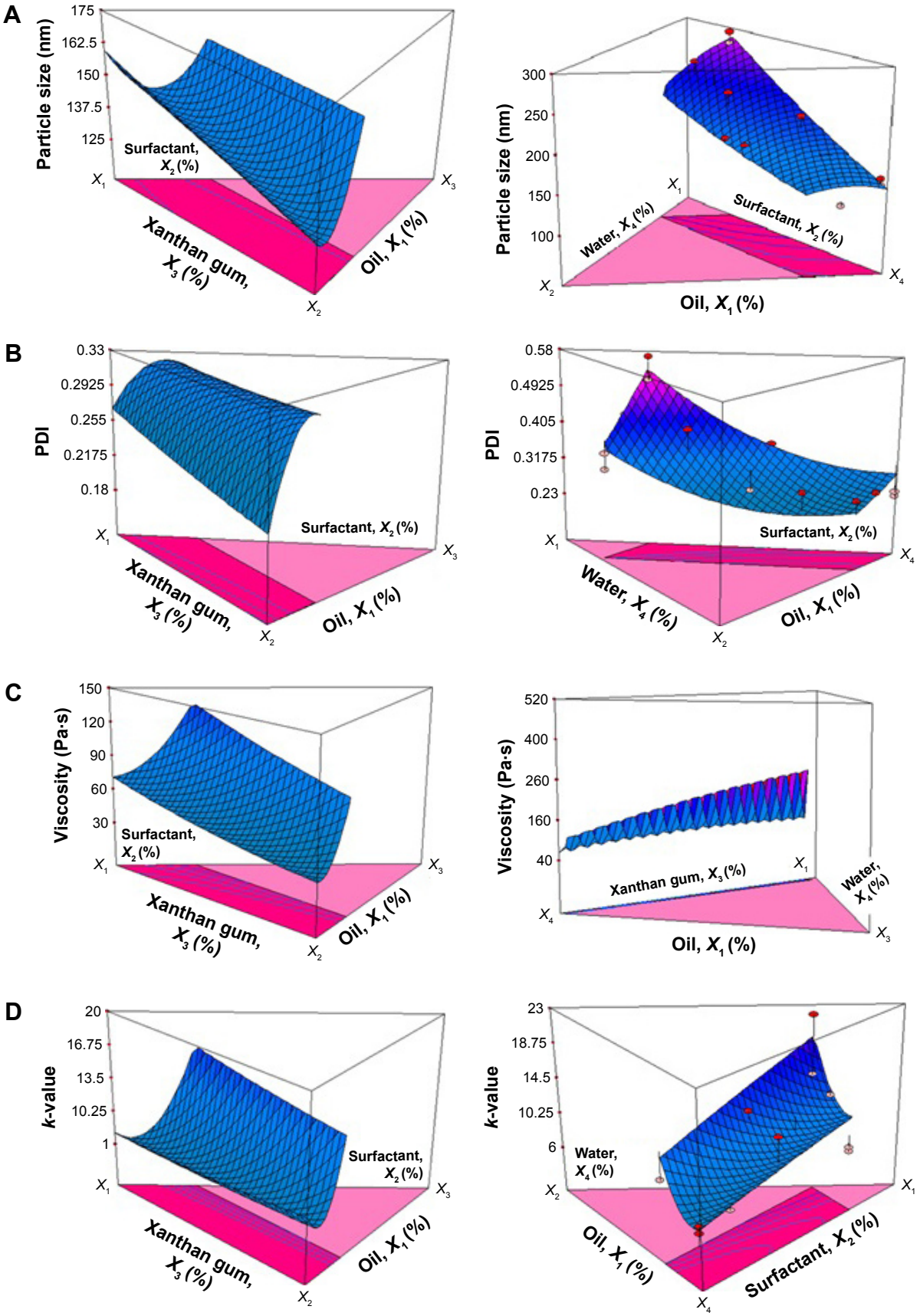

Figure 1 3-D model showing interactions between independent variables.
Note: (**A**) particle size, (**B**) PDI, (**C**) viscosity, and (**D**) *k*-value of nanoemulsion with respect to responses analysis.
Abbreviation: PDI, polydispersity index.

Verification of model

A series of validations was prepared to evaluate the adequacy of the quadratic equation produced by the D-optimal MED analysis. Four random nanoemulsion compositions were formulated to validate the models. Table 4 shows the actual values for all responses studied that were compared with the predicted values.

Optimization of nanoemulsion composition

Table 4 shows that both of the optimized formulations (Opt1 and Opt2) successfully fulfilled the intended values for every response: particle size 100–200 nm, PDI <0.30, viscosity 80–150 Pa·s, and *k*-value >10. Opt1 and Opt2 consisted of 5% and 20% oil content, respectively. Other compositions, such as surfactant, xanthan gum, cyclosporine, and phenonip, were set to be constant. Furthermore, ζ-potential result for each sample was found to be theoretically accepted: <–30 mV. There was no sign of instability (phase separation, creaming, flocculation) after centrifugation analysis (data not shown here). Therefore, it was believed that these two nanoemulsion compositions would possess good stability during storage.

Nanoemulsion pH analysis

A series of nanoemulsions with pH 3.5, 4.5, and 5.5 were prepared, in order to study their stability over time. At 4°C, none of the three nanoemulsions showed any sign of instability throughout the storage period for both Opt1 and Opt2. Nanoemulsions with pH 4.5 and 5.5 were found to be stable without any phase separation or creaming problem for all temperatures (4°C, 25°C, and 45°C). However, at the highest temperature (45°C), it was obvious that the nanoemulsion with pH 3.5 was no longer stable compared to the other two nanoemulsions. A more acidic system consists of a higher degree of H^+ ion. These ions would neutralize the negative charge of the ζ-potential on the droplets' surface, thus reducing repulsion between particles. Uncharged particles promoted droplet flocculation.[42]

At pH 3.5, gravitational separation study showed that about 0%, 33.3%, and 48% of phase creaming occurred for storage at 4°C, 25°C, and 45°C, respectively, for Opt1. Similar results were obtained for Opt2, with 0%, 60%, and 66.7% of gravitational separation at 4°C, 25°C, and 45°C, respectively. The higher the storage temperature, the more unstable the nanoemulsion was, due to the rapid kinetic movement of molecules that led to phase separation. In addition, higher nanoemulsion pH would provide better stability at various temperatures. It has been reported that skin pH <5 results in less scaling of skin and higher hydration compared to pH >5. Skin with eczematous dermatitis is associated with higher skin pH (alkaline condition).[42] Therefore, a stable acidic nanoemulsion (pH 4.5) is a good option in treating an alkaline skin problem.

Stability analysis

The stability of nanoemulsions was a major concern in the formulation study. Table 5 shows the physical stability of Opt1 and Opt2 after centrifugation and after storage at 4°C, 25°C, and 45°C, after 3 months. Both formulations were physically stable, with no creaming, phase separation, or flocculation. However, increments in particle size were observed throughout the 3-month storage as the temperature of storage increased: 4°C (<4% particle-size increment, no significant changes), 25°C (<30% particle-size increment, still in nanosize range), and 45°C (>50% particle-size increment, exceeded nanosize range). Therefore, three analyses were carried out for better understanding the stability of Opt1 and Opt2: coalescence rate, Ostwald ripening, and freeze–thaw cycle.

Coalescence-rate analysis

Coalescence happened when films of continuous phase were ruptured, leading to the fusion of two droplets and forming larger particles. Figure 2 shows the plotted graph of $1/r^2$ versus storage time. According to Equation 4, the plotted graph should show a linear relationship. However, the

Table 4 Validation and optimization sets of cyclosporine-loaded nanoemulsion formulation

	X_1 (%)	X_2 (%)	X_3 (%)	X_4 (%)	R_1 (nm)		R_2		R_3 (Pa·s)		R_4	
					Actual	Predicted	Actual	Predicted	Actual	Predicted	Actual	Predicted
Validation												
V1	22.50	11.00	0.75	64.05	210.00	202.53	0.347	0.344	95.50	96.26	13.41	10.94
V2	25.00	12.50	0.75	60.05	215.70	209.89	0.369	0.346	109.00	99.06	14.66	12.92
V3	24.00	12.50	0.75	61.05	203.80	200.49	0.337	0.331	87.20	95.60	13.19	12.49
V4	22.50	12.50	0.90	62.40	194.50	195.40	0.323	0.311	138.00	127.52	17.80	16.18
Optimization												
Opt1	15.00	15.00	0.75	67.55	116.00	122.53	0.312	0.291	90.10	88.22	10.25	13.79
Opt2	20.00	15.00	0.75	62.55	159.90	155.38	0.269	0.268	132.00	138.69	13.70	15.30

Notes: X_1, particle size; X_2, PDI; X_3, viscosity; X_4, *k*-value of nanoemulsion with respect to responses; R_1, particle size; R_2, PDI; R_3, viscosity; R_4, *k*-value.
Abbreviation: PDI, polydispersity index.

Table 5 Physical stability of optimized nanoemulsion

Formulation	After centrifugation	After 3 months' storage		
		4°C	25°C	45°C
Opt1	✓	✓	✓	✓
Opt2	✓	✓	✓	✓

Note: ✓No phase separation/no creaming.

collected particle-size data did not produce a linear pattern, which indicated no coalescence phenomena in the nanoemulsion system. Therefore, the increment in particle size over time was not caused by coalescence.

Ostwald ripening analysis

Figure 3 shows the Ostwald ripening effect, influenced by different storage temperature and nanoemulsion composition. Storage at 4°C for both nanoemulsions (Opt1 and Opt2) demonstrated excellent stability, with no significant changes in particle size at low Ostwald ripening rate (0.007 nm^3/second and 0.0019 nm^3/second, respectively). Compared to storage at 25°C (0.0778 nm^3/second and 0.3121 nm^3/second, respectively) and 45°C (0.0896 nm^3/second and 0.2913 nm^3/second, respectively), higher storage temperature resulted in higher Ostwald ripening rate. Ostwald ripening was a process in which the particles in the nanoemulsion system underwent expansion to become larger. This phenomenon happened due to the oil-particle diffusion through the continuous phase (water).[43] Particles in the nanoemulsion system absorbed energy from their surroundings. As the temperature increased, the energy of particles increased. The higher the kinetic movement, the higher the possible effective collision between the particles, which led to diffusion among the particles. This promoted particle-size expansion.

Not only was it influenced by storage temperature, Ostwald ripening was also proven to be influenced by oil content. Opt1, with lower oil content, was proven to yield a more stable system compared to the higher oil content in Opt2. The three graphs in Figure 3 show the slope of particle size changing over time. For Opt2, the slope was much steeper than the slope for Opt1. The vertical slope with higher gradient indicated a rapid expansion in particle size. Therefore, Opt1 was more stable over storage for all three temperatures. This can be explained by sufficient surfactant coverage on the particle surfaces, avoiding diffusion among particles.

Freeze–thaw cycle analysis

Under the influence of freezing and thawing cycles, there was no sign of any instability of the nanoemulsion system. After the freeze–thaw cycle, there was only a small change in particle size from the freshly prepared nanoemulsion, with increments of 4.27 nm and 4.97 nm for both Opt1 (initial size 116 nm) and Opt2 (initial size 159.9 nm), respectively. Nanoemulsion appearance remained the same, with no phase separation, creaming, or color change. This finding proved that both optimized nanoemulsions had excellent stability, even after being subjected to the freeze–thaw cycle test.

During freezing, the aqueous phase in the system is crystallized. Freezing and thawing deteriorate the droplets. However, the degree of deterioration is reduced with the help of a small amount of hydrocolloids.[44] In this case, the addition of xanthan gum into the nanoemulsion system helped in maintaining the particle size, as well as the stability of the nanoemulsions.

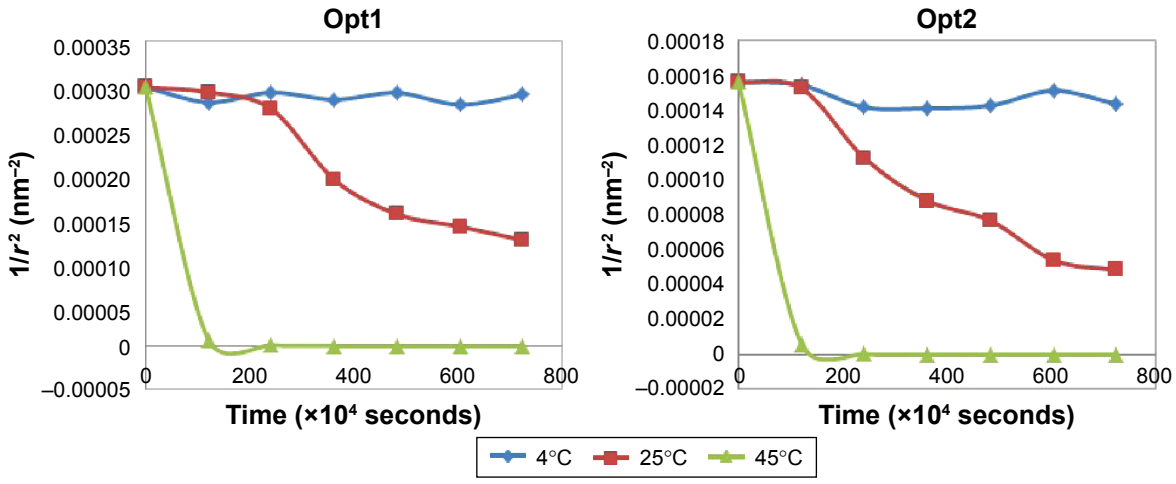

Figure 2 Coalescence rate of Opt1 and Opt2.
Notes: Neither plotted graph exhibits any linear relationship that deviated from the theory of coalescence phenomena. Mean ± standard deviation (n=3).

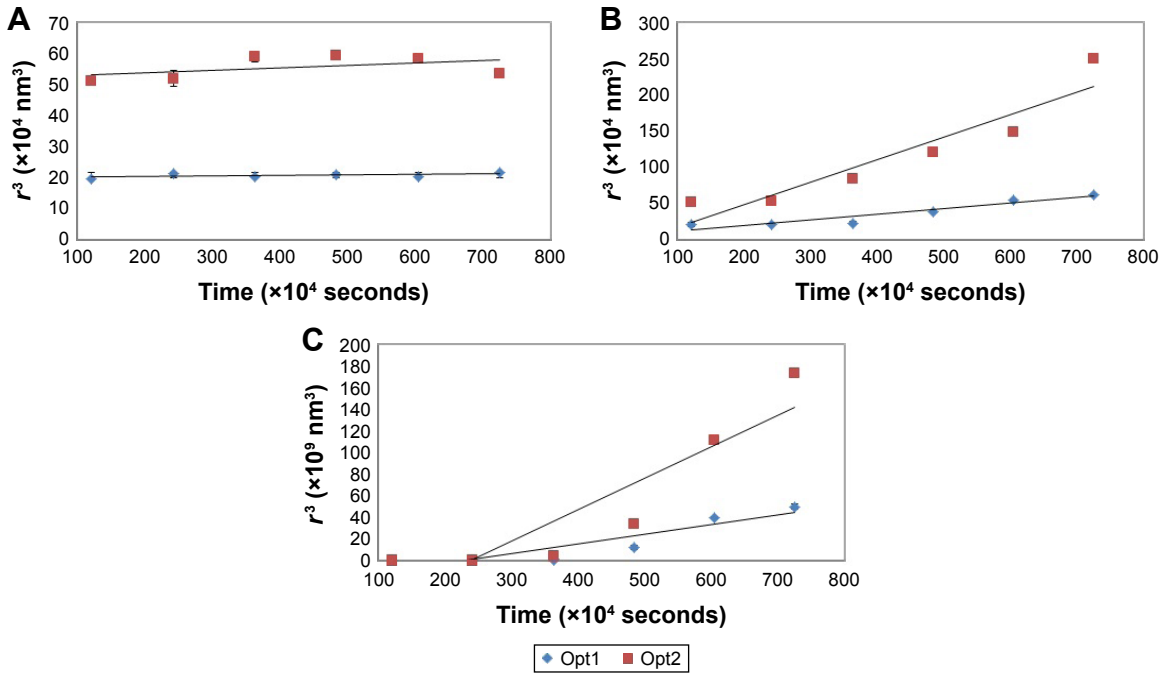

Figure 3 Ostwald ripening stability analysis over 3 months' storage at different temperatures.
Notes: (**A**) 4°C, (**B**) 25°C, and (**C**) 45°C for both optimized nanoemulsions. Mean ± standard deviation (n=3).

In vitro diffusion analysis

Figure 4A shows the percentage of cumulative cyclosporine diffused through the cellulose acetate membrane over 3 hours. Opt2 showed the most efficient diffusion, as it reached 70.48% release within 3 hours of analysis. Opt1 also showed an ability to diffuse 56.12% of the cyclosporine across the membrane within the same period. The same pattern of output was obtained when using the rat skin as a membrane, as illustrated in Figure 4B. Opt2 (97.44%) showed the highest diffusion, followed by Opt1 (81.49%) and the control carrier (72.4%).

The difference between Opt1 and Opt2 was the amount of oil in the composition. Despite the reported effect of thickening agent on diffusion rate,[45] it appeared that the oil content also had a significant effect on the diffusion rate of the drugs. The higher the oil content (Opt2), the faster the diffusion across the membrane. This happened due to the higher number of oil droplets over volume available in the system, which increased the number of droplets carrying cyclosporine successfully crossing the membrane. In addition, cyclosporine-loaded nanoemulsions were proven to give better cyclosporine diffusion compared to the control

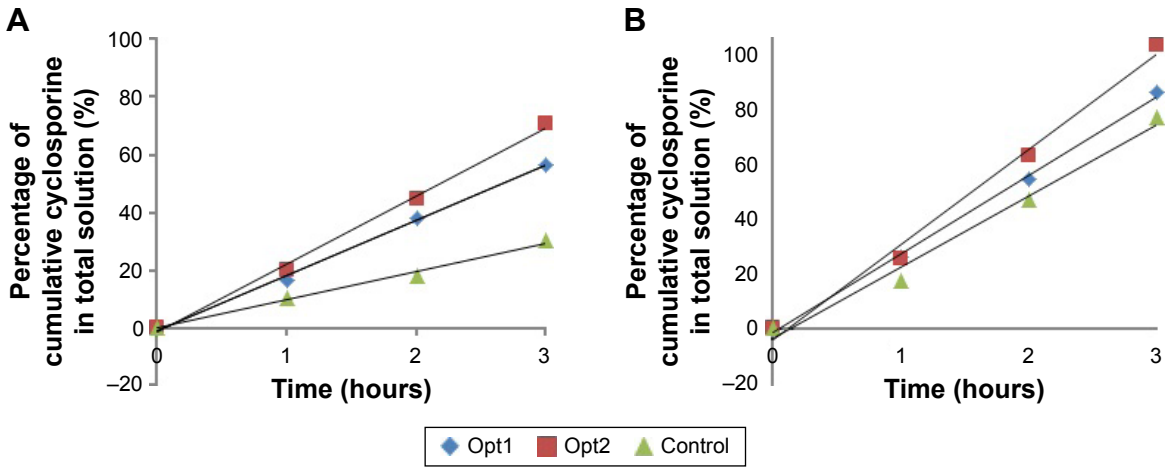

Figure 4 Percentage of cumulative cyclosporine in total solution that successfully diffused through.
Notes: (**A**) Cellulose acetate membrane and (**B**) excised rat-skin membrane within 3 hours of analysis. $P<0.05$ (Opt1 and Opt2 vs control).

Table 6 Correlation coefficients determined by plotted graph corresponding to different kinetic release models

Kinetic model	Coefficient of determination (R^2)	
	Opt1	Opt2
Korsmeyer–Peppas	0.9996	0.9997
Zero-order	0.9979	0.9905
Hixson–Crowell	0.9410	0.9632
First-order	0.9241	0.7981
Higuchi	0.9005	0.8653

sample with ointment carrier. Even though the nature of skin is more favored to lipophilic material, the size of the carrier matters. Better diffusion of cyclosporine was observed when using the nanosize emulsion as a carrier compared to the ointment carrier. With better diffusion, it could provide faster relief to the psoriasis patients.

Synthetic membrane and rat-skin membrane showed similar results for all analyzed samples. However, a difference in diffusion rate was observed. Synthetic membrane is often employed to simulate the skin, because it is hydrophobic and possesses rate-limiting properties like skin.[46] Different membrane types would give different diffusional rates. A similar result was reported by Ng et al, who studied the effect of different membranes on their degree of diffusional properties.[46] Therefore, choosing a suitable membrane is necessary for this application. Excised animal skin is believed to mimic human biology more closely, but it is hard to source and highly inconsistent in quality. Conversely, synthetic membrane is easily sourced, less expensive, and also acts as a quality control.[47] Even though synthetic membranes do not demonstrate any of the perturbation effects that occur in biological samples, the usage of synthetic membranes is preferred, as they are more practical.[46]

Kinetic release analysis

Table 6 shows the coefficient of determination (R^2) for every kinetic model studied, exhibited by Opt1 and Opt2. All the graphs showed linear relationships to different degrees. The highest R^2 value was produced by the Korsmeyer–Peppas model, followed by the zero-order, Hixson–Crowell, first-order, and Higuchi models. The best-fitted model was the Korsmeyer–Peppas model for both Opt1 and Opt2 (0.9996 and 0.9997, respectively). This model illustrated the mechanism of drug diffusion varied as a function of water concentration. Therefore, it explained the difference in release results for Opt1 and Opt2, as the optimized nanoemulsions had different water compositions. The lower the water content in the system, the higher the diffusion, due to the lipophilic property of the membrane used.

In vivo skin analysis

Figure 5A shows average values of TEWL readings from 15 random volunteers. The graph shows a statistically significant change in TEWL reading before and after 3 hours of nanoemulsion application. WL from skin was successfully reduced up to 32.14% and 40.1% by Opt1 and Opt2, respectively. As the TEWL was reduced, water content showed significant improvement. Figure 5B shows the average difference in water content of all volunteers. Application of Opt1 and Opt2 resulted in increments in water content up

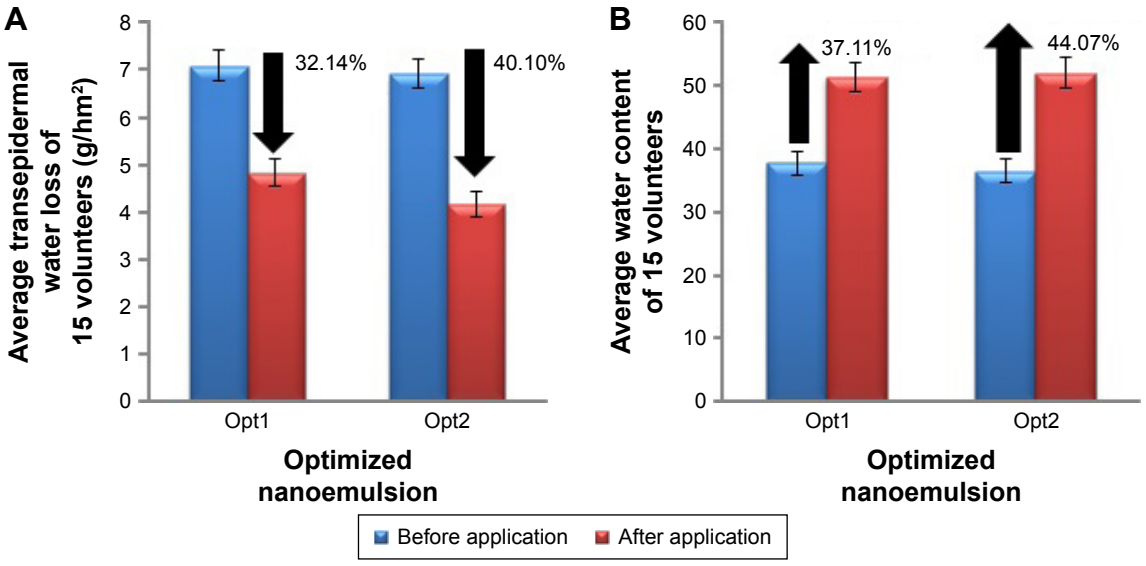

Figure 5 Average differences in (**A**) transepidermal water loss and (**B**) water content.
Notes: Before and after 3 hours of optimized nanoemulsion application in 15 healthy volunteers. Mean ± standard deviation (n=3).

to 37.11% and 44.07%, respectively. This demonstrates a positive result for a good treatment for dry-skin disease.

From the results obtained, Opt2 showed a bigger difference in TEWL and also water-content analysis compared to Opt1. This result was perceived to be majorly influenced by the composition of oil in each nanoemulsion. Opt2 contained 5% extra oil than Opt1. Evangelista et al reported that mineral oil falls under two categories of moisturizer: occlusive and emollient.[25] Occlusive functions by coating the stratum corneum and reducing TEWL, while emollient acts by filling the blanks between desquamating corneocytes to provide cohesion, flattening the curled edges of corneocytes and also giving a smooth surface to the skin.

TEWL is a measurement of the ability of the stratum corneum layer to hold and trap water within corneocytes.[25] The higher the TEWL value, the higher the WL to the surroundings from the stratum corneum. This would lead to a dry-skin problem. Results obtained showed a decrement in TEWL value after 3 hours of application. This indicated that use of the formulated nanoemulsion improved the entrapment of water by the stratum corneum layer and reduced WL. TEWL results corresponded to the hydration of skin. The Corneometer is an instrument that is sensitive to water with a high dielectric constant.[40] Results from the Corneometer represent the skin's water capacitance, which reflects the skin-moisturizing property. As for psoriasis patients, having moisturized skin is one of the main strategies in dealing with itchy skin. As well as successfully lowering TEWL, the formulated nanoemulsion also has the ability to increase water capacitance and hydrate the skin, which would be useful in treating the dry skin of psoriasis patients.

Conclusion

Low-water-soluble cyclosporine with large molecules faced a limitation in the delivery through the topical route. Even though it is currently available as oral therapy for psoriasis, undesired side effects have raised medication awareness. A nanocolloidal carrier (nanoemulsion) was proven to carry this large cyclosporine in its system, and successfully fulfilled the intended physicochemical properties for the topical route. The targeted area for this topical application is focused to reach optimal transdermal diffusion, but with high concentration of cyclosporine in the skin. The 1% cyclosporine-loaded nanoemulsion with intended particle size (100–200 nm) was fabricated with an oil mixture (15%/20%, w/w), Tween 80 as a surfactant (15%, w/w), xanthan gum (0.75%, w/w), water (67.55%/62.55%, w/w), and phenonip as preservative. Both optimum compositions (Opt1 and Opt2) possessed good criteria for a topical nanoemulsion with excellent stability over 3 months of storage. The best temperature for storing the nanoemulsion was 4°C–25°C, as in this range particle size is maintained over time. An increment in size for storage at 45°C was more influenced by Ostwald ripening than the coalescence mechanism. Freeze–thaw analysis showed the nanoemulsion with pH 4.5 to be the minimum in obtaining excellent stability. Nanoemulsions with higher oil content could carry higher cyclosporine content at faster diffusion rate for both rat skin and synthetic membrane, which best fitted the Korsmeyer–Peppas kinetic model. In addition, higher oil content possessed a better effect on TEWL and moisture content of the skin.

Disclosure

The authors report no conflicts of interest in this work.

References

1. Rahman M, Alam K, Ahmad MZ, et al. Classical to current approach for treatment of psoriasis: a review. *Endocr Metab Immune Disord Drug Targets*. 2012;12:287–302.
2. Schön MP, Boehncke WH. Psoriasis. *N Engl J Med*. 2005;352:1899–1912.
3. Bremmer S, Voorhees AS, Hsu S, et al. Obesity and psoriasis: from the medical board of the National Psoriasis Foundation. *J Am Acad Dermatol*. 2010;63:1058–1069.
4. Georgiou KR, Scherer MA, Fan CM, et al. Methotrexate chemotherapy reduces osteogenesis but increases adipogenic potential in the bone marrow. *J Cell Physiol*. 2012;227:909–918.
5. Rosenberg P, Urwitz H, Johannesson A, et al. Psoriasis patients with diabetes type 2 are at high risk of developing liver fibrosis during methotrexate treatment. *J Hepatol*. 2007;46:1111–1118.
6. Winterfield LS, Menter A, Gordon K, Gottlieb A. Psoriasis treatment: current and emerging directed therapies. *Ann Rheum Dis*. 2005;64:87–92.
7. Stähelin HF. The history of cyclosporin A (Sandimmune) revisited: another point of view. *Experientia*. 1996;52:5–13.
8. Italia JL, Bhardwaj V, Kumar MN. Disease, destination, dose and delivery aspects of ciclosporin: the state of the art. *Drug Discov Today*. 2006;11:846–854.
9. Puigdemont A, Brazís P, Ordeix L, et al. Efficacy of a new topical cyclosporine A formulation in the treatment of atopic dermatitis in dogs. *Vet J*. 2013;197:280–285.
10. Rezzani R, Buffoli B, Rodella L, Stacchiotti A, Bianchi R. Protective role of melatonin in cyclosporine A-induced oxidative stress in rat liver. *Int Immunopharmacol*. 2005;5:1397–1405.
11. Gisondi P, Cazzaniga S, Chimenti S, et al. Metabolic abnormalities associated with initiation of systemic treatment for psoriasis: evidence from the Italian Psocare Registry. *J Eur Acad Dermatol Venereol*. 2012;27:e30–e41.
12. Honeywell-Nguyen PL, Bouwstra JA. Vesicles as a tool for transdermal and dermal delivery. *Drug Discovery Today Technol*. 2005;2:67–74.
13. Burroni AG, Fassino M, Torti A, Visentin E. How do disease perception, treatment features, and dermatologist-patient relationship impact on patients assuming topical treatment? An Italian survey. *Patient Relat Outcome Meas*. 2015;6:9–17.
14. Lebwohl M, Ting PT, Koo JY. Psoriasis treatment: traditional therapy. *Ann Rheum Dis*. 2005;64:83–87.
15. Feldman SR, Horn EJ, Balkrishnan R, et al. Psoriasis: improving adherence to topical therapy. *J Am Acad Dermatol*. 2008;59:1009–1016.

16. Malik IA, Akhter S, Kamal MA. Treatment of psoriasis by using *hijamah*: a case report. *Saudi J Biol Sci*. 2015;22:117–121.
17. Zahir H, Nand RA, Brown KF, Tattam BN, Mclachlan AJ. Validation of methods to study the distribution and protein binding of tacrolimus in human blood. *J Pharmacol Toxicol*. 2001;46:27–35.
18. Salim N, Ahmad N, Musa SH, Rauzah H, Tadros TF, Basri M. Nano-emulsion as a topical delivery system of antipsoriatic drugs. *RSC Adv*. 2016;6:6234–6250.
19. Pey CM, Maestro A, Solé I, González C, Solans C, Gutiérrez JM. Optimization of nano-emulsions prepared by low-energy emulsification methods at constant temperature using a factorial design study. *Colloids Surf A Physicochem Eng Asp*. 2006;288:144–150.
20. Kumar KK, Sasikanth K, Sabareesh M, Dorababu N. Formulation and evaluation of diacerein cream. *Asian J Pharm Clin Res*. 2011; 4:93–98.
21. Shivakumar HN, Murthy SN. Topical and transdermal drug delivery. In: Kulkarni VS, editor. *Handbook of Non-Invasive Drug Delivery Systems*. Oxford, UK: Elsevier; 2010:1–36.
22. Machmudah S, Sulaswatty A, Sasaki M, Goto M, Hirose T. Supercritical CO_2 extraction of nutmeg oil: experiments and modeling. *J Supercrit Fluids*. 2006;39:30–39.
23. Sonavane GS, Sarveiya VP, Kasture VS, Kasture SB. Anxiogenic activity of *Myristica fragrans* seeds. *Pharmacol Biochem Behav*. 2002;71: 239–244.
24. Marina AM, Man YB, Nazimah SA, Amin I. Chemical properties of virgin coconut oil. *J Am Oil Chem Soc*. 2009;86:301–307.
25. Evangelista MT, Abad-Casintahan F, Lopez-Villafuerte L. The effect of topical virgin coconut oil on SCORAD index, transepidermal water loss, and skin capacitance in mild to moderate pediatric atopic dermatitis: a randomized, double-blind, clinical trial. *Int J Dermatol*. 2014; 53:100–108.
26. Nevin KG, Rajamohan T. Effect of topical application of virgin coconut oil on skin components and antioxidant status during dermal wound healing in young rats. *Skin Pharmacol Physiol*. 2010;23:290–297.
27. Cafaggi S, Leardi R, Parodi B, Caviglioli G, Bignardi G. An example of application of a mixture design with constraints to a pharmaceutical formulation. *Chemometr Intell Lab Syst*. 2003;65:139–147.
28. Petrovic A, Cvetkovic N, Ibric S, et al. Application of mixture experimental design in the formulation and optimization of matrix tablets containing carbomer and hydroxy-propylmethylcellulose. *Arch Pharm Res*. 2009;32:1767–1774.
29. Gao P, Witt MJ, Haskell RJ, Zamora KM, Shifflett JR. Application of a mixture experimental design in the optimization of a self-emulsifying formulation with a high drug load. *Pharm Dev Technol*. 2005;9:301–309.
30. Anarjan N, Mirhosseini H, Baharin BS, Tan CP. Effect of processing conditions on physicochemical properties of astaxanthin nanodispersions. *Food Chem*. 2010;123:477–483.
31. Masoumi HR, Basri M, Samiun WS, Izadiyan Z, Lim CJ. Enhancement of encapsulation efficiency of nanoemulsion-containing aripiprazole for the treatment of schizophrenia using mixture experimental design. *Int J Nanomedicine*. 2015;10:6469–6476.
32. Tang SY, Manickam S, Wei TK, Nashiru B. Formulation development and optimization of a novel Cremophore EL-based nanoemulsion using ultrasound cavitation. *Ultrason Sonochem*. 2012;19:330–345.
33. Wooster TJ, Golding M, Sanguansri P. Impact of oil type on nano-emulsion formation and Ostwald ripening stability. *J Am Chem Soc*. 2008;24:12758–12765.
34. Han NS, Basri M, Rahman MB, Rahman RN, Salleh AB, Ismail Z. Phase behavior and formulation of palm oil esters o/w nanoemulsions stabilized by hydrocolloid gums for cosmeceuticals application. *J Dispers Sci Technol*. 2011;32:1428–1433.
35. Thanasukarn P, Pongsawatmanit R, McClements DJ. Utilization of layer-by-layer interfacial deposition technique to improve freeze-thaw stability of oil-in-water emulsions. *Food Res Int*. 2006;39:721–729.
36. Singhvi G, Singh M. Review: in vitro drug release characterization models. *Int J Pharm Stud Res*. 2011;2:77–84.
37. Jafari SM, He Y, Bhandari B. Production of sub-micron emulsions by ultrasound and microfluidization techniques. *J Food Eng*. 2007;82: 478–488.
38. Musa SH, Basri M, Masoumi HR, et al. Formulation optimization of palm kernel oil esters nanoemulsion-loaded with chloramphenicol suitable for meningitis treatment. *Colloids Surf B Biointerfaces*. 2013; 112:113–119.
39. Huang X, Kakuda Y, Cui W. Hydrocolloids in emulsions: particle size distribution and interfacial activity. *Food Hydrocoll*. 2001;15: 533–542.
40. Lapasin R, Grassi M, Coceani N. Effects of polymer addition on the rheology of o/w microemulsions. *Rheol Acta*. 2001;40:185–192.
41. Samson S, Basri M, Masoumi HR, Karjiban RA, Malek EA. Design and development of a nanoemulsion system containing copper peptide by D-optimal mixture design and evaluation of its physicochemical properties. *RSC Adv*. 2016;6:17845–17856.
42. Lambers H, Piessens S, Bloem A, Pronk H, Finkel P. Natural skin surface pH is on average below 5, which is beneficial for its resident flora. *Int J Cosmet Sci*. 2006;28:359–370.
43. Chang Y, McLandsborough L, McClements DJ. Fabrication, stability and efficacy of dual-component antimicrobial nanoemulsions: essential oil (thyme oil) and cationic surfactant (lauric arginate). *Food Chem*. 2015; 172:298–304.
44. Pongsawatmanit R, Srijunthongsiri R. Influence of xanthan gum on rheological properties and freeze-thaw stability of tapioca starch. *J Food Eng*. 2008;88:137–143.
45. Salim N, Basri M, Rahman MB, Abdullah DK, Basri H. Modification of palm kernel oil esters nanoemulsions with hydrocolloid gum for enhanced topical delivery of ibuprofen. *Int J Nanomedicine*. 2012;7: 4739–4747.
46. Ng SF, Rouse J, Sanderson D, Eccleston G. A comparative study of transmembrane diffusion and permeation of Ibuprofen across synthetic membrane using Franz diffusion cells. *Pharmaceutics*. 2010;2: 209–223.
47. Ng SF, Rouse JJ, Sanderson FD, Meidan V, Eccleston GM. Validation of static Franz diffusion cell system for in vitro permeation studies. *AAPS PharmSciTech*. 2010;11:1432–1441.